Hindawi
Journal of Nanomaterials
Volume 2022, Article ID 6331372, 9 pages
https://doi.org/10.1155/2022/6331372

Research Article

Prediction of Tensile Shear Fracture Load of Friction Stir Spot-Welded AA2024-T3/HCS Dissimilar Joints

Vishnu G. Nair,[1] Gujar Anant Kumar Jotiram,[2] Kumar Pratyush,[3] Bhasker Pant,[4] D. Raja Ramesh,[5] Amara S. A. L. G. Gopala Gupta,[6] L. H. Manjunatha,[7] S. Madhavarao,[8] and Sintayehu Mekuria Hailegiorgis[9]

[1]*Department of Aeronautical and Automobile Engineering, Manipal Institute of Technology, Manipal Academy of Higher Education (MAHE), 576104, Manipal, Karnataka, India*
[2]*Department of Mechanical Engineering, D. Y. Patil College of Engineering and Technology, Kolhapur, Maharashtra 416006, India*
[3]*Department of Pharmaceutical Chemistry, SVKM's Institute of Pharmacy, Dhule, Maharashtra 424001, India*
[4]*Department of Computer Science & Engineering, Graphic Era Deemed to be University, Dehradun, Uttarakhand 248002, India*
[5]*Department of Mechanical Engineering, Sri Vasavi Institute of Engineering and Technology, Nandamuru (Krishna District), 521369 Andhra Pradesh, India*
[6]*Department of Computer Science and Engineering, Koneru Lakshmaiah Education Foundation, Vaddeswaram, 522502 Andhra Pradesh, India*
[7]*School of Mechanical Engineering, REVA University, Bangalore, 560064 Karnataka, India*
[8]*Department of Mechanical Engineering, Sagi Rama Krishnam Raju Engineering College (A), Bhimavaram, Andhra Pradesh 534204, India*
[9]*Certer of Excellence for Bioprocess and Biotechnology, Department of Chemical Engineering, College of Biological and Chemical Engineering, Addis Ababa Science and Technology University, Addis Ababa, Ethiopia*

Correspondence should be addressed to Sintayehu Mekuria Hailegiorgis; sintayehu.mekuria@aastu.edu.et

Received 19 March 2022; Revised 9 April 2022; Accepted 19 April 2022; Published 27 May 2022

Academic Editor: Samson Jerold Samuel Chelladurai

Lightweight materials play a vital role in many industries because of their weight reduction, corrosion resistance, and formability. On the other hand, joining this alloy is a very tedious process for everyone in industries due to incompatibility in metallurgical properties. The thick intermetallic formation, porosity, and segregation of alloys in the weld are the possible causes during welding of dissimilar materials by the fusion welding process. Nowadays, these materials have been joined by solid-state welding friction stir welding. AA2024 and high carbon steel (HCS) were used for friction stir spot welding in this investigation. Tool rotational speed, plunge rate, plunge depth, and dwell time were the major influencing process parameters. Design of experiments and response surface methodology were used to optimize the process parameters to attain maximum lap shear strength of AA2024/HCS.

1. Introduction

AA2024 and high carbon steel (HCS) are the most prevalent materials in heavy structural fabrication industries because of their availability, formability, machinability, etc. [1]; these two alloys are high-strength materials that possess unique properties like corrosion resistance, strength, and light-weight material [2]. The only problem with these materials is that joining materials is very difficult in the fusion welding process due to metallurgical incompatibility [3]. Hence, it is a significant challenge for welding and manufacturing engineers. Nowadays, these two alloys are welded using a solid-state welding process, friction stir welding (FSW). In some of the areas like fabrication, aircraft structure uses riveted

Table 1: Chemical composition of BM.

Material	C	Cu	Mn	Mg	S	V	Zr	Ti	Sn	Zn	Al	Fe
2024-T3	—	4.3	0.5	1.3	—	0.05	0.12	0.02	0.04	0.01	Bal.	—
AISI-1095	0.9	—	0.4		0.04	—	—	—	—	—	—	Bal.

Table 2: Mechanical characterization of BM.

Material	YS (MPa)	UTS (MPa)	Elongation (%)	Microhardness (HV)
2024-T3	315	455	9	135
AISI-1095	460	830	10	245

Table 3: Feasible working limits of process parameters.

Parameters	Limits	Defects
N (rpm)	$N < 600$	Due to low heat generation in sufficient material flow
	$N > 1400$	High heat input resulted in severe plastic deformation
R (mm/min)	$R < 8$	Insufficient material flow resulted in poor bonding
	$R > 24$	Excess flash-key hole defect
T (sec)	$T < 3$	Lack of dwell time causes insufficient bonding of the material
	$T > 7$	More dwell time causes key hole formation
D	$D < 1.5$	Heat generation low-insufficient material flow
	$D > 3.5$	High heat input and more distortion

Table 4: Important FSSW parameters and their levels.

Sl. No	Factor	Unit	Levels				
			-2	-1	0	+1	+2
1	N	rpm	800	900	1000	1100	1200
2	R	mm/min	2	3	4	5	6
3	T	Sec	3	4	5	6	7
4	D	—	2.0	2.5	3.0	3.5	4.0

joints [4]. By the use of rivets, the payload of the aircraft increases; also, corrosion takes place between two dissimilar materials (galvanic coupling) [5]. Friction stir spot welding is a modified version of the FSW process. This is the most familiar process for replacing riveted joints in all structural fabrication. Bozkurt and Bilici [6] used Taguchi to find optimal FSSW process parameters on AA2024-AA5754 dissimilar alloy. L9 orthogonal array was used to optimize the parameters, and the position of the palate was the primary influencing parameter, among others. Ahmed et al. [7] carried out FSW of AA2024-AISI1018 different alloy. A continuous layer of intermetallic was formed at high temperatures. This layer was found to be the most predominant location for fracture.

Moreover, the fracture mode was found to be mixed mode. Yang et al. [8] reviewed the mechanical and metallurgical properties of FSSW joints. The review concluded that the FSSW is the potential process to join dissimilar materials. Lyu et al. [9] investigated the effect of double-sided FSSW on the shear fracture load of aluminum alloy and steel sheet. The shear force of the FSSW joints increased with increasing plunge force. Ojo et al. [10] reviewed the latest trend in FSSW on similar and dissimilar materials. The investigation studied the material flow in the nugget zone and shoulder diameter effect on weld nugget formation. Siddharth and Senthilkumar [11] optimized FSSW parameters of AA2024-C 1100 dissimilar materials using response surface methodology (RSM). Analysis of variance (ANOVA) was used to identify the individual parameter effect on shear fracture load. The maximum shear fracture load was obtained using RSM. Colmenero et al. [12] used the vibration signal's energy to optimize FSSW parameters of Al-Cu dissimilar joints. Two significant parameters, such as rotational speed and dwell time, were used, and RSM predicted

Table 5: DoE of FSSW joints.

Exp. No.	Coded value				SFL of Al/steel joint (kN)
	N	*T*	*R*	*D*	
1	-1	-1	-1	-1	6.33
2	+1	-1	-1	-1	6.75
3	-1	+1	-1	-1	6.90
4	+1	+1	-1	-1	7.73
5	-1	-1	+1	-1	7.29
6	+1	-1	+1	-1	7.41
7	-1	+1	+1	-1	7.65
8	+1	+1	+1	-1	8.21
9	-1	-1	-1	+1	6.95
10	+1	-1	-1	+1	7.45
11	-1	+1	-1	+1	7.48
12	+1	+1	-1	+1	8.26
13	-1	-1	+1	+1	7.82
14	+1	-1	+1	+1	8.41
15	-1	+1	+1	+1	8.31
16	+1	+1	+1	+1	8.40
17	-2	0	0	0	6.12
18	+2	0	0	0	7.21
19	0	-2	0	0	7.06
20	0	+2	0	0	8.44
21	0	0	-2	0	8.39
22	0	0	+2	0	9.76
23	0	0	0	-2	5.87
24	0	0	0	+2	6.85
25	0	0	0	0	9.46
26	0	0	0	0	9.13
27	0	0	0	0	9.18
28	0	0	0	0	9.07
29	0	0	0	0	9.28
30	0	0	0	0	9.37

maximum shear fracture load. Aita et al. [13] optimized the FSSW of AA6060 aluminum alloy using Taguchi and full factorial design. The quadratic equation was developed to correlate the process parameters and strength. Taguchi and complete factorial design were used to optimize the process parameters. Habibizadeh et al. [14] investigated the optimum shear strength of friction stir spot welding parameters of AA1050/C10100. The primary and interaction of FSSW parameters were obtained by analysis of variance. Zhang et al. [1] investigated the multiobjective optimization of friction stir spot-welded parameters on aluminum alloy sheets. NSGA-II method was selected to determine the Pareto front and subsequently choose the best possible solutions.

Many researchers throughout the globe have used DOE to improve FSSW parameters in both similar and dissimilar alloys, different Al alloys [14], and aluminum-steel [15]. However, no attempt has yet been made to construct empirical correlations to forecast the ability of aluminum and carbon steel joints to bear tensile shear fracture load-carrying capacities. This study is aimed at building a mathematical relationship to forecast shear fracture load of FSSW dissimilar joints.

2. Experimental Work

In this investigation, 2 mm thick AA2024 and 2 mm thick high carbon steel were chosen as the base materials, whose chemical and mechanical properties are presented in Tables 1 and 2, respectively. Samples were cut into the required size (25 mm width and 75 mm length) using a do-all machine followed by cleaning burrs and removed by the buffing wheel. The samples were washed with acetone to remove the scale and rust formation on the piece.

Table 3 presents the feasible range of each process parameter. The impact of primary process parameters on shear fracture load of AA2024/HCS dissimilar materials was evaluated. In this work, the following process parameters such as diameter ratio (shoulder to pin diameter) (*D*), rotational speed (*R*), plunge rate (*R*), and dwell time (*T*) were identified from the previous work. The feasible range of each process parameter was fixed based on the joint that would get free from visual defects.

The lower limit and upper limit of each process parameter were set as +2 and -2, respectively [16]. The intermediate value of each process parameter was calculated using the below mentioned equation:

$$X_i = \frac{2[2X - (X_{\max} + X_{\min})]}{(X_{\max} - X_{\min})}. \quad (1)$$

Table 4 shows the specified process parameters together with their limitations.

Table 5 displays the chosen design matrix. The microstructure of base materials is shown in Figures 1(a) and 1(b). Similarly, the photograph of the welding machine is shown in Figure 1(c). Super HSS material was used to make tools with five different shoulder diameters (Figure 1(d)). The diameter and length of the pins were both kept at 5 mm. On the pin, a tapered threaded (left hand) profile was created. With the use of an automatic controlled FSW machine, all of the trials were carried out under the circumstances stipulated by the design matrix. Aluminum test coupon was kept at the bottom, and steel test coupon was placed on the top sheet. The photograph of the fabricated joint before testing and after testing is shown in Figures 1(e) and 1(f), respectively.

3. Development of Empirical Relationship

TSFL response (*Y*) of Al/steel FSSW joints (Equation (2)) may be described as a function of *N*, *R*, *T*, and *D*.

$$Y = f(N, R, T, D). \quad (2)$$

The chosen factor and its influence are presented in the

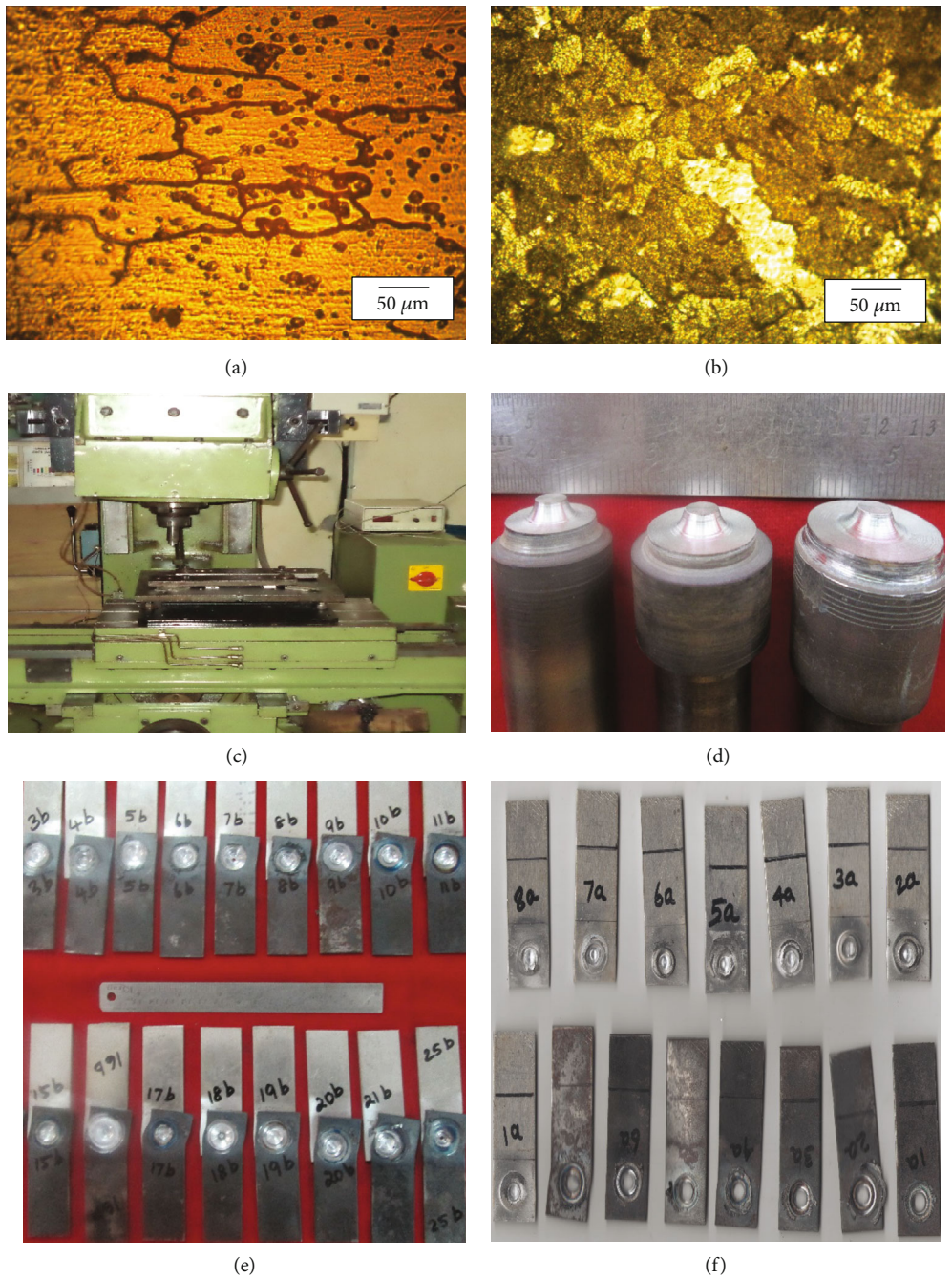

Figure 1: Optical micrograph of (a) AA7075 and (b) HCS; photograph of (c) FSW machine, (d) fabricated tool, (e) fabricated joints (before the test), and (f) fabricated joints after the test.

following equation:

$$Y = b_0 + b_1 * N + b_2 * R + b_3 * T + b_4 * D + b_{11} * N^2 + b_{22} * R^2 + b_{33} * T^2 + b_{44} * D^2 + b_2 * N * R + b_{13}[N * T] + b_{14}[N * D] + b_{23}[R * T] + b_{24}[R * D] + b_{34}[T * D]. \quad (3)$$

The values of these coefficients were calculated using Design Expert 9.1. The final empirical connection to predict TSFL was built using these coefficients once the coefficients were determined [17], and the generated empirical relationship is shown in the following equation:

$$\text{TSFL} = 9.25 + 0.25 * N + 0.30 * R + 0.35 * T + 0.28 * D + 0.039(N * R) - 0.073\,(N * T) - 0.078\,(R * T) - 0.056\,(R * D) - 0.63 * N^2 - 0.35 * R^2 - 0.023 * T - 0.70 * D^2\ \text{kN}. \quad (4)$$

The appropriateness of the generated empirical

Table 6: ANOVA test results.

Source	Squares	df	Sum of square	P value	Prob > F	
Model	31.87	14	2.28	186.65	<0.0001	Significant
N	1.54	1	1.54	58.45	<0.0001	
T	2.93	1	2.93	111.66	<0.0001	
R	2.21	1	2.21	84.30	<0.0001	
D	1.91	1	1.91	72.70	<0.0001	
$N * T$	0.086	1	0.086	3.26	0.0912	
$N * R$	0.025	1	0.025	0.94	0.3466	
$R * T$	0.098	1	0.098	3.72	0.0730	
$N * D$	5.6E-5	1	5.6E-5	2.1E-3	0.9637	
$T * D$	1.5E-4	1	1.5E-4	5.9E-3	0.9395	
$R * D$	0.050	1	0.050	1.88	0.1900	
R^2	3.44	1	3.44	131.06	<0.0001	
N^2	10.73	1	10.73	408.58	<0.0001	
D^2	13.51	1	13.51	514.26	<0.0001	
T^2	0.015	1	0.015	0.55	0.4684	
Residual	0.39	15	0.026			
Lack of fit	0.28	10	0.028	1.27	0.4170	Nonsignificant
Pure error	0.12	5	0.021			
Cor. total	32.26	29				
Std. dev.	0.16		Calc. R^2	0.9878		
Mean	7.88		Adj. R^2	0.9764		
C.V. (%)	2.06		Pred. R^2	0.9445		
Prec.	1.78		Adeq. Prec.	33.514		

Table 7: Confirmation results.

Expt. No.	N (rpm)	R (mm/min)	T (sec)	D	TSFL (kN) Actual	TSFL (kN) Predicted	Error (%)
1	1015	4.3	6	3	9.45	9.51	-0.6
2	1020	4.2	6	3	9.64	9.68	-0.4
3	1030	4.5	6	3	9.62	9.48	+1.4

relationship was examined using the analysis of variance (ANOVA) approach [18]. The ANOVA findings are shown in Table 6.

The model has an F value of 185.56, indicating that it is noteworthy. The F value of a model this big has a 0.01% probability of occurring due to noise. The model terms are important if the "Prob > F" value is less than 0.050. N, R, T, D, TN, TR, DR, DT, R^2, N^2, T^2, and D^2 are important model terms in this situation. The corrected R^2 value of is equally high, at 0.97, indicating the model's high relevance. The corrected R^2 of 0.97 agrees reasonably with the expected R^2 of 0.94, showing that the model may be utilized to forecast the TSFL. The S-N ratio is used to determine adequate accuracy, and a ratio of more than 4 is preferred. Because this model's precession is 34.714. The observed and projected response values are nearly identical, indicating a near-perfect match of the derived empirical connection. Fabricating FSSW joints with three random combinations of parameters in the test range validates the proposed empirical connection; the actual response was determined as the average of three measured results. The validation findings indicated that the empirical connection created is extremely accurate, with a forecast variation of less than 5% (Table 7).

4. Optimizing FSSW Parameters

The mechanical and metallurgical qualities of the joints are influenced by FSSW process parameters such as N, R, T, and D. In order to achieve exceptional mechanical qualities, the FSSW process parameters must be optimized. RSM is one of the most effective approaches for optimizing the FSSW process parameters. RSM [19] is a set of mathematical and statistical models that may be used to investigate and simulate engineering challenges [20]. To graphically depict the region of best factor settings, a contour map is created.

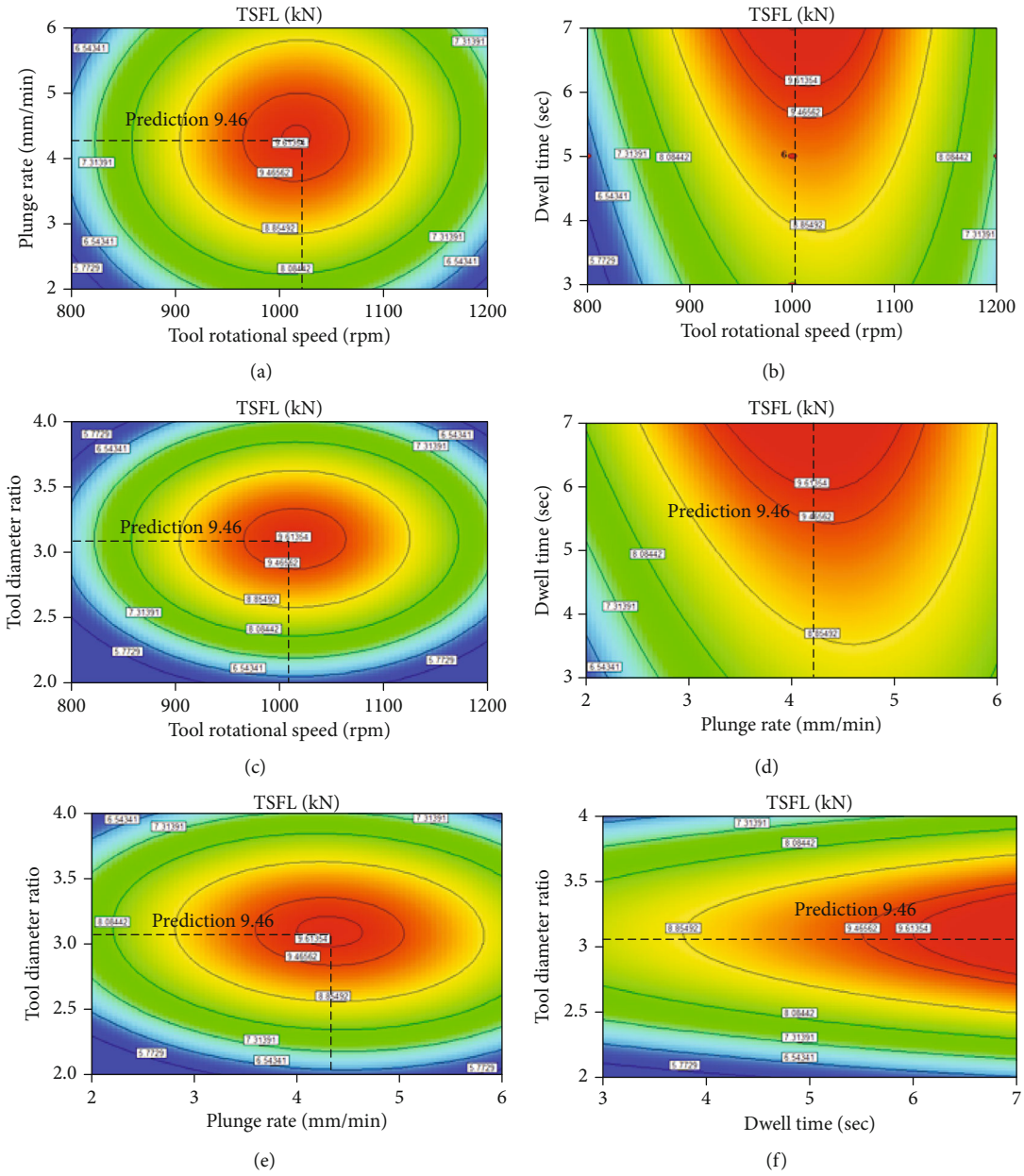

Figure 2: (a–f) Contour plots showing the interaction effects between parameters in Al/steel joints.

The contour plots' characteristic circular mound form indicates that the elements are more likely to be interdependent [21]. A plot like this for second-order response surfaces might be more complicated than a simple set of parallel lines for first-order models. It is frequently important to define the response surface in the immediate region of the stationary point after it has been located. Characterization involves deciding if the discovered stationary point is the greatest, lowest, or saddle point. A contour plot is used to discover this. In the examination of the response surface, contour plots are quite useful. The optimum is determined with reasonable precision by defining the form of the surface using contour plots generated with response surface analysis software. If a circular contour patterning occurs, it likely to imply factor independence, but elliptical contours may show factor interactions. The forecasting model' response surfaces were created by taking two middle-level parameters and putting them on the "X"- and "Y"-axes, with the response plotted on the "Z"-axis. We can see the ideal response point on the response surfaces. The contour plots and response graphs for the model developed for the FSSW of 2024-T3 with carbon steel alloy are shown in Figures 2 and 3.

5. Analysis of Contour Plots and Response Surface Plots

The contour plot in Figure 2 clearly shows the beneficial interaction impact of tool rotational speed and plunge rate on tensile shear failure load (a). Changes in the tensile shear failure load are more sensitive to changes in tool rotating speed than

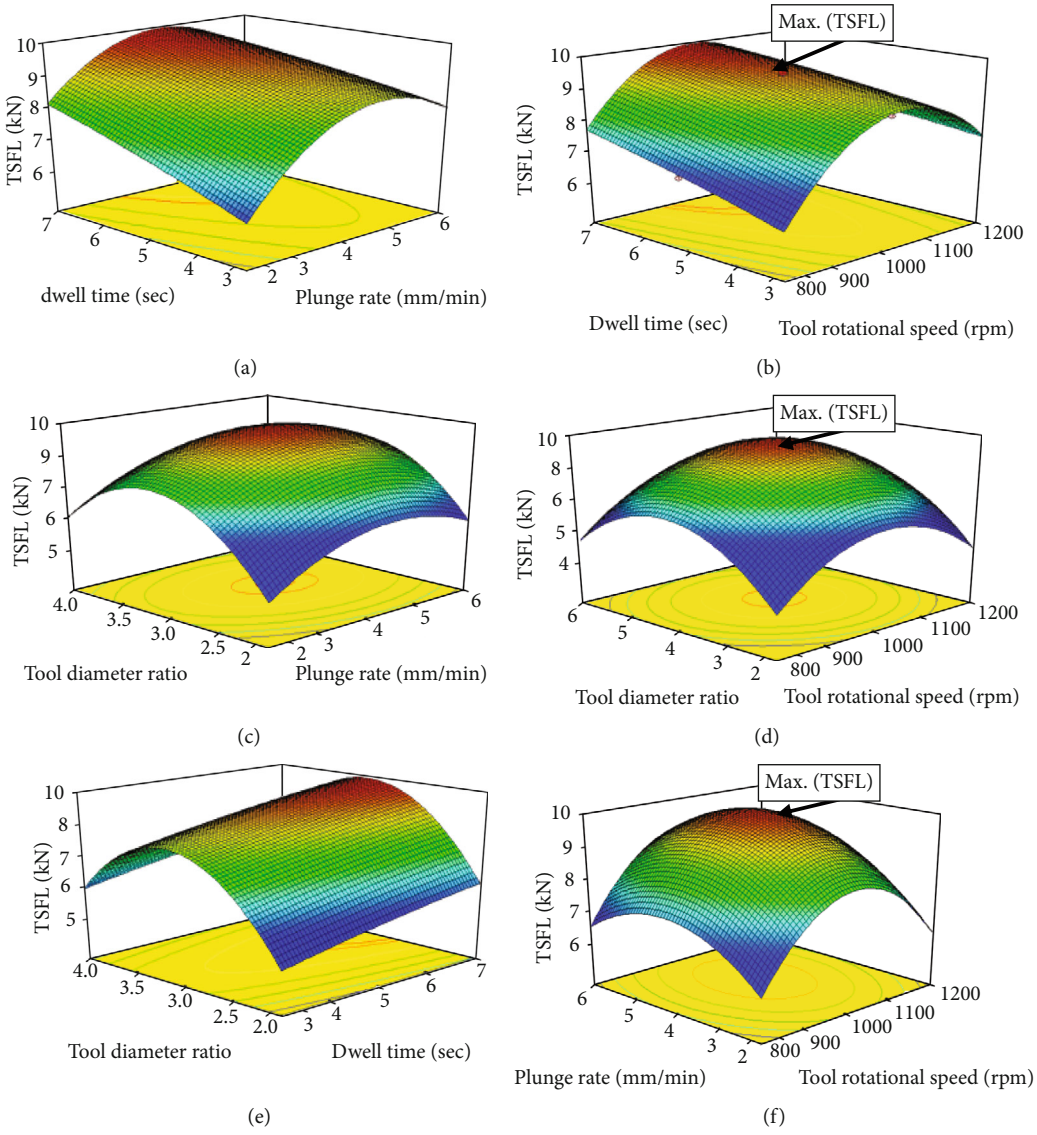

Figure 3: (a–f) Response surface graphs showing the optimal point for Al/steel joints.

to changes in dwell time, as seen in the contour plot in Figure 2(b). Despite the virtually circular shape of Figure 2(c), there is a little interaction between tool rotating speed and tool diameter ratio, and it is believed that dwell time has a bigger impact on TSFL than tool rotational speed. As seen in the contour plot (Figure 2), dwell duration has a stronger impact on TSFL than plunge rate. The interaction effects between the parameters, plunge rate, and tool diameter ratio, on tensile shear failure load are also substantial, as shown in the contour plot Figure 2(e). As demonstrated in Figure 2, changes in dwell time are more sensitive to changes in TSFL than changes in tool diameter ratio. Figure 3 shows the three-dimensional response surface plots for the generated regression model's response (TSFL). The TSFL is shown by the apex of the response surface [22]. The TSFL increases with increasing tool rotational speed, plunge rate, and dwell duration to a certain value and subsequently declines, as shown in Figure 3. It is also noticed that increasing the tool diameter ratio initially raises the TSFL, but future increases have no meaningful influence on the TSFL. The highest attainable TSFL value is discovered to be 9.46 kN after examining the response surfaces and contour plots (Figures 2 and 3). With a tool speed of 999.21 rpm, a plunge rate of 3.91 mm/min, a dwell time of 4.98 seconds, and a tool diameter ratio of 3.01, achievers' optimization approach was validated by fabricating three more joints. Table 7 displays the welding settings as well as the TSFL findings.

6. Conclusions

The dissimilar materials such as AA2024 and HCS are welded successfully using FSSW. From the experimental investigation, the following conclusions are drawn:

(1) The experiments were conducted using the design of experiments; four-factor, five-level central rotatable composite matrix was used

(2) The joint welded with rotational tool speed, plunge depth, dwell time, and shoulder diameter to pin diameters was 1000 rpm, 4 mm/min, 5 sec, and 3, respectively

(3) The significance of each process parameter was identified using ANOVA; from the analysis, dwell time is the primary influencing parameter, followed by plunge rate, shoulder diameter to pin diameter ratio, and rotational speed

(4) The maximum tensile shear fracture load of FSSW dissimilar joints was found to be 9.46 kN

(5) The joint yielded a higher TSFL value than other joints, which may be forming an intermetallic compound by optimum heat input

Data Availability

The data used to support the findings of this study are included within the article.

Conflicts of Interest

The authors declare that they have no conflicts of interest.

References

[1] B. Zhang, X. Chen, K. Pan, and J. Wang, "Multi-objective optimization of friction stir spot-welded parameters on aluminum alloy sheets based on automotive joint loads," *Metals*, vol. 9, no. 5, p. 520, 2019.

[2] Q. Chu, W. Y. Li, X. W. Yang et al., "Microstructure and mechanical optimization of probeless friction stir spot welded joint of an Al-Li alloy," *Journal of Materials Science & Technology*, vol. 34, no. 10, pp. 1739–1746, 2018.

[3] L. Zhou, L. Y. Luo, R. Wang, J. B. Zhang, Y. X. Huang, and X. G. Song, "Process parameter optimization in refill friction spot welding of 6061 aluminum alloys using response surface methodology," *Journal of Materials Engineering and Performance*, vol. 27, no. 8, pp. 4050–4058, 2018.

[4] S. Jannet, P. Koshy Mathews, and R. Raja, "Optimization of process parameters of friction stir welded AA 5083-O aluminum alloy using response surface methodology," *Bulletin of the Polish Academy of Sciences: Technical Sciences*, vol. 63, no. 4, pp. 851–855, 2015.

[5] G. H. Li, L. Zhou, F. Y. Shu, and Y. C. Liu, "Statistical and metallurgical analysis of dissimilar friction stir spot welded aluminum/copper metals," *Journal of Materials Engineering and Performance*, vol. 29, no. 3, pp. 1830–1840, 2020.

[6] Y. Bozkurt and M. K. Bilici, "Application of Taguchi approach to optimize of FSSW parameters on joint properties of dissimilar AA2024-T3 and AA5754-H22 aluminum alloys," *Materials & Design*, vol. 51, pp. 513–521, 2013.

[7] M. M. Z. Ahmed, N. Jouini, B. Alzahrani, M. M. Seleman, and M. Jhaheen, "Dissimilar friction stir welding of AA2024 and AISI 1018: microstructure and mechanical properties," *Metals*, vol. 11, no. 2, p. 330, 2021.

[8] X. W. Yang, T. Fu, and W. Y. Li, "Friction stir spot welding: a review on joint macro- and microstructure, property, and process modelling," *Advances in Materials Science and Engineering*, vol. 2014, 11 pages, 2014.

[9] X. Lyu, M. Li, X. Li, and J. Chen, "Double-sided friction stir spot welding of steel and aluminum alloy sheets," *The International Journal of Advanced Manufacturing Technology*, vol. 96, no. 5-8, pp. 2875–2884, 2018.

[10] O. O. Ojo, E. Taban, and E. Kaluc, "Friction stir spot welding of aluminum alloys: a recent review," *Materials Testing*, vol. 57, no. 7-8, pp. 609–627, 2015.

[11] S. Siddharth and T. Senthilkumar, "Optimization of friction stir spot welding process parameters of dissimilar Al 5083 and C 10100 joints using response surface methodology," *Russian Journal of Non-ferrous Metals*, vol. 57, no. 5, pp. 456–466, 2016.

[12] A. N. Colmenero, M. S. Orozco, E. J. Macías et al., "Optimization of friction stir spot welding process parameters for Al-Cu dissimilar joints using the energy of the vibration signals," *The International Journal of Advanced Manufacturing Technology*, vol. 100, no. 9-12, pp. 2795–2802, 2019.

[13] C. A. Aita, I. C. Gracioli, T. Góss, M. D. de Souza Rosendo, A. W. Tier, and A. Reguly, "Shear strength optimization for FSSW AA6060-T5 joints by Taguchi and full factorial design," *Journal of Materials Research and Technology*, vol. 9, no. 6, pp. 16072–16079, 2020.

[14] A. Habibizadeh, M. Honarpisheh, and S. I. Golabi, "Determining optimum shear strength of friction stir spot welding parameters of AA1050/C10100 joints," *Manufacturing Technology*, vol. 21, no. 3, pp. 315–329, 2021.

[15] R. Suryanarayanan and V. G. Sridhar, "Effect of process parameters in pinless friction stir spot welding of Al 5754-Al 6061 alloys," *Metallography, Microstructure, and Analysis*, vol. 9, no. 2, pp. 261–272, 2020.

[16] C. Rajendran, K. Srinivasan, V. Balasubramanian, H. Balaji, and P. Selvaraj, "Data set on prediction of friction stir welding parameters to achieve maximum strength of AA2014-T6 aluminium alloy joints," *Data in Brief*, vol. 23, p. 103735, 2019.

[17] C. Rajendran, K. Srinivasan, V. Balasubramanian, H. Balaji, and P. Selvaraj, "Identifying combination of friction stir welding parameters to maximize strength of lap joints of AA2014-T6 aluminium alloy," *Australian Journal of Mechanical Engineering*, vol. 17, no. 2, pp. 64–75, 2019.

[18] C. Rajendran, K. Srinivasan, V. Balasubramanian, H. Balaji, and P. Selvaraj, "Identifying the combination of friction stir welding parameters to attain maximum strength of AA2014-T6 aluminum alloy joints," *Advances in Materials and Processing Technologies*, vol. 4, no. 1, pp. 100–119, 2018.

[19] I. T. Abdullah and S. K. Hussein, "Improving the joint strength of the friction stir spot welding of carbon steel and copper using the design of experiments method," *Multidiscipline Modeling in Materials and Structures*, vol. 14, no. 5, pp. 908–922, 2018.

[20] S. M. Goushegir, J. F. Dos Santos, and S. T. Amancio-Filho, "Influence of process parameters on mechanical performance and bonding area of AA2024/carbon-fiber-reinforced

poly(phenylene sulfide) friction spot single lap joints," *Materials & Design*, vol. 83, pp. 431–442, 2015.

[21] R. N. Verastegui, J. A. E. Mazzaferro, C. C. P. Mazzaferro, T. R. Strohaecker, and J. F. D. Santos, "Welding of aluminum to DP600 steel plates by refill friction stir spot welding process (refill FSSW): preliminary results," *Advanced Materials Research*, vol. 1082, pp. 123–132, 2014.

[22] G. N. ShivaKumar and G. Rajamurugan, "Friction stir welding of dissimilar alloy combinations—a review," *Proceedings of the Institution of Mechanical Engineers, Part C: Journal of Mechanical Engineering Science*, vol. 1, p. 09544062211069292, 2022.